GLIA

GLIA 58:1949–1960 (2010)

A Proteome Map of Axoglial Specializations Isolated and Purified from Human Central Nervous System

AJIT S. DHAUNCHAK,[1]* JEFFREY K. HUANG,[1,2] OMAR DE FARIA JUNIOR,[1] ALEJANDRO D. ROTH,[1,3] LILIANA PEDRAZA,[1] JACK P. ANTEL,[1] AMIT BAR-OR,[1] AND DAVID R. COLMAN[1]*

[1]*The Montreal Neurological Institute (MNI) and Hospital, McGill University and the McGill University Health Centre, Department of Neurology and Neurosurgery, Program in NeuroEngineering of McGill University, 3801 University Avenue, Montreal H3A2B4, Canada*

[2]*Department of Veterinary Medicine, University of Cambridge, Cambridge, United Kingdom*

[3]*Department of Biology, University of Chile, Santiago, Chile*

KEY WORDS

myelin; node of Ranvier; myelin inhibition; multiple sclerosis; white matter disorder

ABSTRACT

Compact myelin, the paranode, and the juxtaparanode are discrete domains that are formed on myelinated axons. In humans, neurological disorders associated with loss of myelin, including Multiple Sclerosis, often also result in disassembly of the node of Ranvier. Despite the importance of these domains in the proper functioning of the CNS, their molecular composition and assembly mechanism remains largely unknown. We therefore performed a large-scale proteomics MudPIT screen for the identification of proteins in human myelin and axogliasomal fractions. We identified over 1,000 proteins in these fractions. Since even minor perturbations in neuron-glial interactions can uncouple the glial support of axons, the proteome map presented here can be used as a reference library for "myelin health" and disease states, including white matter disorders such as leukodystrophies and multiple sclerosis.

INTRODUCTION

Myelin ensheathment by oligodendrocytes (OL) in the human central nervous system (CNS) ensures rapid impulse conduction. In addition to insulation, myelin has also been shown to trigger domain formation on the axon (Pedraza et al., 2001; Poliak and Peles, 2003). Myelinated axonal segments (internodes) are flanked by short unmyelinated segments (nodes of Ranvier). Voltage-gated sodium channels are clustered at these nodes, limiting depolarization to this sharply demarcated zone; as a result, action potentials "jump" from one node to the next. The region immediately flanking the node is termed the paranode and the outermost domain is called the juxta-paranode. For simplicity, we have termed the axonal specializations together with the overlying and attached glial paranodal loops as the "axoglial apparatus" (Huang et al., 2005; Pedraza et al., 2001). How these microdomains are assembled is a major focus of research efforts.

Genetic perturbations resulting in white matter abnormalities are eventually lethal in humans, often progressively diminishing the ability to perform even the simplest motor tasks. Several animal models, either genetically-engineered or carrying spontaneous mutations, mimic human white matter disorders. These conditions have shed light on the underlying pathology of several leukodystrophies, including Pelizeaus-Merzbacher disease (PMD), X-linked Adrenoleukodystrophy (ALD), 18q Syndrome (*shiverer mice*), Metachromatic Leukodystrophy (MLD). However, the underlying causes of demyelinating (e.g., multiple sclerosis) versus dysmyelinating ailments (e.g., leukodystrophies) remain poorly understood. In addition, why mutations in certain housekeeping genes like eukaryotic initiation factor 2 family proteins (eIF2B α-to-gamma) or genes associated with peroxisomal disorders result in white matter loss is still unclear. A better understanding of the underlying mechanisms of disease requires generation of the proteome and transcriptome map of human OLs and myelin, as has been attempted for rodents (Dugas et al., 2006; Roth et al., 2006; Taylor and Pfeiffer, 2003; Taylor et al., 2004; Vanrobaeys et al., 2005; Werner et al., 2007; Yamaguchi et al., 2008). Accordingly, we modified the myelin-isolation protocol and purified myelin and axogliasomes from freshly dissected human white matter tissue. The axoglial structures are remarkably stable and retain junctional morphology upon extraction with high concentration detergent. We performed a large-scale nongel-based proteome screen on the biochemically-isolated fractions. We identified over 750 proteins in the human myelin fraction and over 450 in the axo-

Additional Supporting Information may be found in the online version of this article.

Grant sponsors: Rio Tinto Alcan, The Molson Foundation, The Myelin Repair Foundation, Center of Excellence Award [(2007) Government of Canada], MS Society of Canada Postdoctoral Fellowship.

*Correspondence to: Ajit S. Dhaunchak, The Montreal Neurological Institute (MNI) and Hospital, McGill University and the McGill University Health Centre, Department of Neurology and Neurosurgery, Program in NeuroEngineering of McGill University, 3801 University Avenue, Montreal H3A2B4, Canada. E-mail: ajit.dhaunchak@mcgill.ca and David R. Colman, The Montreal Neurological Institute (MNI) and Hospital, McGill University and the McGill University Health Centre, Department of Neurology and Neurosurgery, Program in NeuroEngineering of McGill University, 3801 University Avenue, Montreal H3A2B4, Canada. E-mail: david.colman@mcgill.ca

Received 26 March 2010; Accepted 22 July 2010

DOI 10.1002/glia.21064

Published online 9 September 2010 in Wiley Online Library (wileyonlinelibrary.com)

glial fraction. When comparing the myelin proteome library to that of the axoglial compartment, we found overlapping but distinct proteomes. We identified proteins of diverse classes including metabolic, biosynthesis, and degradation machineries. The proteome map presented here is much larger than previously determined in murine counterparts and we report over 400 proteins that were not known to be components of myelin. We also present a proteome map of the axoglial fraction with over 400 proteins that were not described previously (Huang et al., 2005). The proteome map presented here may include novel autoantigens in multiple sclerosis, disease-associated proteins in the discrete OL domains, and novel molecules inhibiting regeneration in the CNS. The human proteome map presented here thus can be used as an atlas for myelin health and disease.

MATERIALS AND METHODS

Antibodies and Reagents

Monoclonal mouse obtained from following sources: anti-PSD-95 (K28/43) and anti-panNeurofascin (A12/18) from Neuromab, anti-Actin (A1978 Sigma), anti-Gfap (G-9269 Sigma), anti-Gapdh (G8795 Sigma), anti-Tubulin (AA12.1 Hybridoma Bank, Iowa), claudin-11/OSP (a gift of Dr. Alexander Gow, Wayne State University, Detroit, MI), anti-sodium channel (K58/35 Sigma), anti-PLP clone 3F4 (Dhaunchak and Nave, 2007). Polyclonal rabbit were anti-Caspr (Tait et al., 2000), anti-Calnexin (3811-100 Biovision), anti-CNP (Bernier et al., 1987), anti-OMgp (H-222 SantaCruz), anti-14-3-3 (K-19 SantaCruz), anti-MAG (Salzer et al., 1987), anti-MBP (Pedraza et al., 1997), Adam23 (a gift of Dr. Charles ffrench-Constant, Cambridge University, Cambridge, UK), Crmp-2 (a gift of Dr. Jerome Honnorat, INSERM U433, France), plasmolipin (a gift of Dr. Victor Sapirstein, The Nathan Klein Institute, Orangeburg, NY), All chemicals and reagents used were from Sigma.

Isolation and Purification of Myelin and Axoglial Apparatus Fractions

We obtained myelin from human tissue excised from surgical resections carried out to ameliorate nontumor-related intractable epilepsies (ages 20–45 years) at the Montreal Neurological Institute. Tissues used were from regions requiring resection to reach the precise epileptic focus, and were distant from the main electrically active site. The protocol was approved by an institutional review board according to the guidelines provided by the Canadian Institutes for Health Research. Tissue was homogenized in HB (0.32 M sucrose, 1 mM MgCl, 10 mM Tris-HCl (pH 7.5), 0.1 mM PMSF) on ice with a motorized Teflon homogenizer. The molarity of homogenate was adjusted to 1.25 M sucrose, by addition of 2.0 M sucrose. Homogenate was then layered with 1 and 0.32 M sucrose containing 20 mM Tris-HCl (pH 7.5), and 0.1 mM PMSF. After a 100,000*g* overnight centrifugation at 4°C, the 0.32/1.0 M interface (crude myelin membranes), and 1.0/1.25 M interface (axogliasomes) were collected, diluted 1:1 with ice cold H_2O and pelleted at 100,000*g* for 1 h to concentrate the membranes. The axogliasomes and myelin fractions were hypoosmotically shocked by homogenization in 20 vol. of ice cold H_2O, containing 20 mM Tris pH 7.5 and 0.1 mM PMSF, incubated for 30 min on ice and rehomogenized. The shocked membranes were pelleted at 40,000*g* for 20 min, resuspended in 0.32 M sucrose and refloated to respective interfaces by ultracentrifugation at 100,000*g* for 3 h. The collected membranes were shocked once again before pelleting, and recovered for subsequent experiments.

Immunoblotting

Equal amounts of protein resolved on denaturing SDS-gel were transferred to PVDF membranes (Millipore). The membranes were rinsed briefly in TBST (25 mM Tris pH 7.4, 27 mM KCl, 137 mM NaCl, 0.1% Tween 20) and blocked for at least 1 h at room temperature in blocking buffer (5% nonfat dry milk in TBST). Primary antibody diluted in blocking buffer was applied for at least 1 h at room temperature (or overnight at 4°C). After four washes in TBS-T, HRP-conjugated secondary antibodies were applied for 45 min, washed four times in TBS-T and developed using Enhanced Chemiluminescence Detection kit (PerkinElmer).

Immunohistochemistry

CNS tissues were obtained from postnatal day 18 rat spinal cords or brains after intercardial perfusion with 4% PFA, cryo-protected through a 12, 15, and 20% sucrose series and embedded by rapid freezing in Tissue Tek OCT for cryosectioning. For sodium channel staining, the rats were perfused transcardially via 4% paraformaldehyde filled 30-cm^3 syringes for no more than 5 min, and dissected tissues were postfixed for another 5–10 min before cryoprotection. Longitudinal and transverse sections (15 μm) were generated and placed on Superfrost/Plus glass slides (Fisher), and stored at −80°C until use. PNS tissues were obtained from P18 rat sciatic nerves, fixed for 15 min in 4% paraformaldhyde, transferred to 1X PBS, cut longitudinally, transferred to a drop of 1X PBS on a Superfrost/Plus glass slide. The perineurium was stripped and removed, and the nerve was teased with No. 5 superfine forceps (Roboz). The teased fibers were dried and stored in −80°C until use. For immunofluorescence, the slides containing CNS or PNS tissue sections were rinsed in 1X PBS for 5 min, blocked for 1 h in blocking solution (5% normal goat serum, 0.2% Tx-100 in 1X PBS), hybridized with primary antibodies in the blocking solution overnight, washed with 1X PBS, and incubated with species specific secondary antibodies conjugated to Cy2, Cy3, or Cy5 in blocking solution for 60 min. The sections were washed three times in 1X PBS for 10 min each and mounted in mounting medium (50 mM Tris, pH 8.6, 2.5% DABCO, 90% glycerol). The sections were examined with an Olympus FV1000 laser scanning confocal microscope.

Thin Section Electron Microscopy

The collected myelin membranes and axogliasomes were pelleted by centrifugation at 15,000 rpm in 4°C for 20 min prior to fixation with 4% glutaraldehyde. For detergent extraction, axogliasomes were extracted (v/v) with final concentration of either 0.1 or 1.0% Tx 100 containing 20 mM Tris-HCl at pH 7.5, and 0.1 mM PMSF, mixed and incubated on ice for 30 min. The detergent insoluble pellets were obtained after centrifugation in 15,000 rpm at 4°C for 30 min. The collected myelin fractions, axogliasomes, and detergent insoluble axogliasomes were then fixed with 4% glutaraldehyde in 1X PBS, pH 7.5 for 2 h on ice. The fixed pellets were subsequently washed with 1X PBS for 5 min, treated with 2% osmium tetroxide in cacodylate buffer, pH 7.5, dehydrated through an ethanol series, and embedded in epon (Embed 812, Electron Microscopy Sciences). Ultrathin sections were generated and collected on copper grids. Each grid was treated with uranyl acetate-lead citrate staining, and examined with a JEOL electron microscope.

Multidimensional Protein Identification Technology

The human myelin fraction was resuspended in 0.1% SDS, digested in trypsin and subjected to MudPIT analysis at the W.M. Keck Facility (Yale University). The LC-MS/MS spectra were subjected to amino-acid composition analysis either by MASCOT or SEQUEST algorithms. The data obtained is from two samples over three runs, where more than 1,000 proteins were detected, of which around 770 were considered to be the most reliable identifications (at least two unique peptides to the protein in question). For the myelin samples, the raw data was pooled and about 70% of the proteins were common to both samples. The human axogliasomal fractions were subjected to MudPIT analysis and 46 relevant proteins were previously described (Huang et al., 2005). To be considered as a candidate for axoglial apparatus or myelin library identification at least two unique peptides was required for previously unknown proteins whereas only a single peptide was considered sufficient if the protein was a known component of the respective axoglial specialization.

RESULTS

Preservation of Myelin Structure and Intact Axoglial Junctions in Isolated Fractions

To compare the proteomes of the myelin domains, we first purified these fractions. We exploited the high lipid-to-protein ratio of myelin to biochemically isolate myelin membranes and associated axogliasomal fractions from human white matter (HWM). Because of the lipid content, the compact myelin membranes can easily be segregated from other membranes and organelles by flotation on a high density sucrose cushion via ultracentrifugation (Norton and Poduslo, 1973). Since axogliasomes contain a much higher protein-to-lipid ratio than compact myelin, these membranes can easily be sheared away from compact myelin and recovered at a higher isopycnic density (Huang et al., 2005). By using a discontinuous sucrose gradient during ultracentrifugation, both fractions are simultaneously enriched at different interfaces, depleting one from the other. These fractions were first examined by thin section electron microscopy to verify the abundance of multilayered membranes and intact paranodal structures. Multilayered myelin-like membranes were readily seen in myelin fractions (Fig 1A), and the axogliasomal fraction was mainly composed of membrane-limited "sacs" ranging from 250 to 500 nm (Fig. 1B,C) corresponding to disrupted but still recognizable paranodal loops. Paranodal membranes sheared away from compact myelin during homogenization and stably associated with one another and the axolemma despite the intensely disruptive shearing forces exerted during homogenization (Huang et al., 2005). White matter also contains an abundance of nonparanodal membranes derived from nonmyelinating glial cell types such as astrocytes. Therefore, to remove astrocytic membranes as well as loosely bound axolemmal fragments and soluble cytoplasmic components (Norton and Poduslo, 1973), we osmotically shocked the axogliasomes, refloated the membranes at the 1.0/1.25 M sucrose interface, and further extracted the recovered membranes with a non-ionic detergent (0.1% Tx-100). Thin section electron microscopy of the resulting axogliasomes revealed a further enrichment of isolated axoglial junctions held together by fragments of paranodal

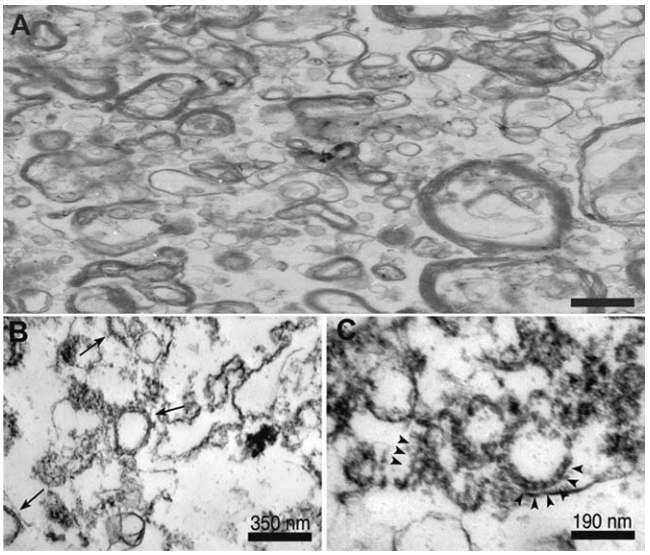

Fig. 1. Axoglial and myelin membranes are enriched in isolated fractions. Myelin and axogliasome fractions were pelleted and processed for thin section electron microscopy. (**A**) Electron micrograph from the human myelin fraction shows that the enriched fraction is mainly composed of myelin-like membranes. (**B**, **C**) Prior to processing for thin section electron microscopy, the mouse axogliasome fraction was extracted with 0.1% TritonX-100 and pelleted. Most detergent-extracted axogliasomes consisted of glial vesicles attached to axolemmal fragments (arrows). (C) Magnification of such glial vesicles demonstrates distinct septate particles (arrowheads) in the isolated axoglial junctions.

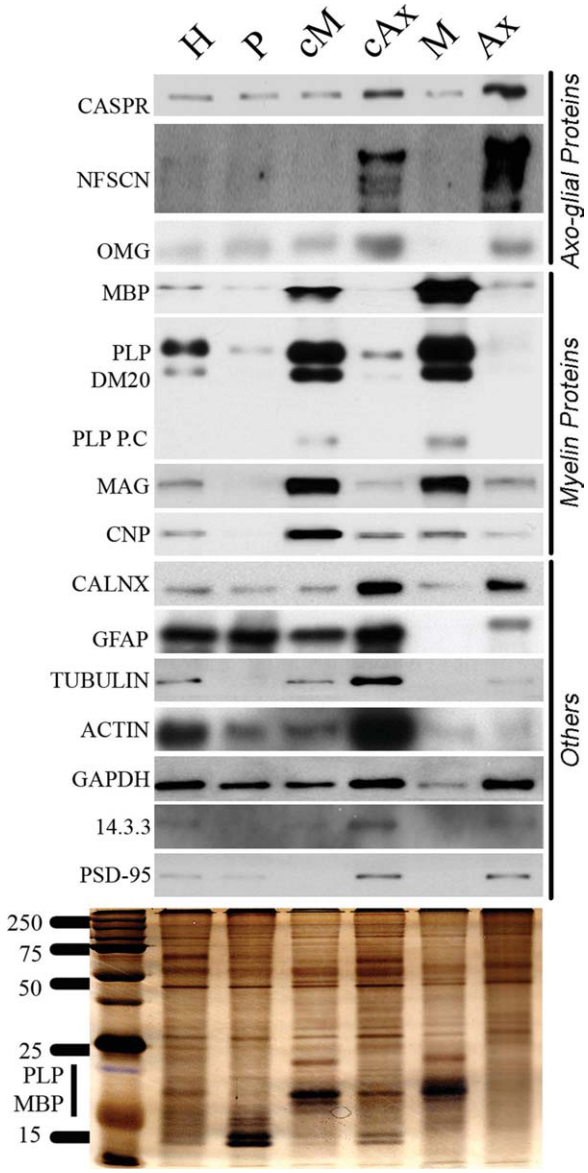

Fig. 2. Reciprocal proteomes in human axoglial specializations. Human white matter homogenized in 0.32 M sucrose (H) was subjected to discontinuous sucrose density ultracentrifugation. Two interfaces obtained after the first ultracentrifugation are mainly composed of crude myelin (cM) and crude axogliasome (cAx) fractions. To obtain pure myelin (M) and axogliasomes (Ax), crude fractions were subjected to osmotic shocks. All fractions, including the pellet (P) obtained after the first centrifugation, were resolved on a 4–20% gradient gel and transferred to PVDF membrane. The membranes were probed for proteins that are known components of the axoglial-apparatus or myelin including the nodal/paranodal proteins CASPR, NFSCN, and OMgp, and myelin proteins MBP, PLP/DM20 and proteolytic products (P.C). Other proteins that are proposed as components of myelin and axoglial apparatus are also shown. In addition, 5 μg protein from each fraction was resolved on gradient gels, fixed, and silver stained. Note that PLP/DM20 and MBP make up the majority of myelin proteins, these proteins are virtually depleted from axogliasomal fractions.

and axolemmal membranes (Fig. 1B,C). Intact septate densities of ~15 nm in length were readily detected in the axoglial junction fragments. Even under high detergent extraction conditions (1.0% Triton-X 100), when most of the plasma membrane was removed, axoglial junctions remained insoluble and yet preserved the septate densities across the cleft (Supp. Info. Fig. 1). The axoglial junction is therefore remarkably stable and is likely to function as an intermembrane adhesive structure, although the molecular basis for adhesion *in situ* still remains to be determined.

Reciprocal Protein Representation in Isolated Myelin and Axoglial Fractions

We next determined if known components of myelin and paranode were enriched in the fractions as compared with HWM homogenates. Western blot analysis demonstrated that nodal/paranodal proteins including CASPR, NFSCAN, and OMGP were clearly enriched in the axogliasomal fraction (see Fig. 2) when compared with the HWM lysate or myelin fraction. Conversely, compact myelin proteins PLP, DM20, PLP/DM20 proteolytic products, MBP, and CNP were highly enriched in the myelin fraction but were not significantly present in axogliasomal fractions. Another OL-specific protein (MAG), which is present at the periaxolemmal channel of compact myelin as well as in the paranodal loops (Trapp et al., 1989), was detected in both the compact myelin and axogliasomal fractions. These results further reveal a notable separation of paranodal axoglial membranes from compact myelin by cell fractionation. In addition to myelin- and nodal/paranodal-specific proteins, we also probed these fractions for the presence of proteins proposed as components of myelin including CALNEXIN, GAPDH, TUBULIN, ACTIN, 14-3-3. These proteins were significantly enriched in axoglial fractions, suggesting that the detection of some of these components in myelin could be due to leakage from paranodal loops (see Fig. 2).

Dissecting the Molecular Composition of Human Myelin and Axogliasomal Fractions

Myelin and axogliasomal fractions were subjected to multidimensional protein identification technology (MudPIT) mass spectroscopy (MS) analysis. MudPIT is not subject to the same bias as gel-based screens and detects peptides of all isoelectric points, molecular weights, and hydrophobicities, including those that are integral membrane and low-abundance proteins. The proteome map of human myelin included 770 proteins. We identified several classical and recently documented as well as several hundred previously undescribed proteins. Transcripts for some of these are exclusively expressed by mature OLs (Cahoy et al., 2008; Dugas et al., 2006), suggesting a specialized function in myelin. Identification of other ubiquitous proteins suggests their role in functions common to other neural cells. Several known rodent myelin membrane proteins, including hydrophobic membrane and basic proteins that remain undetectable while using gel-based assays were readily detected with MudPIT analysis. These include MOBP, TMEM10, NECLs, IGSF8, MAL2, and others (Bello-

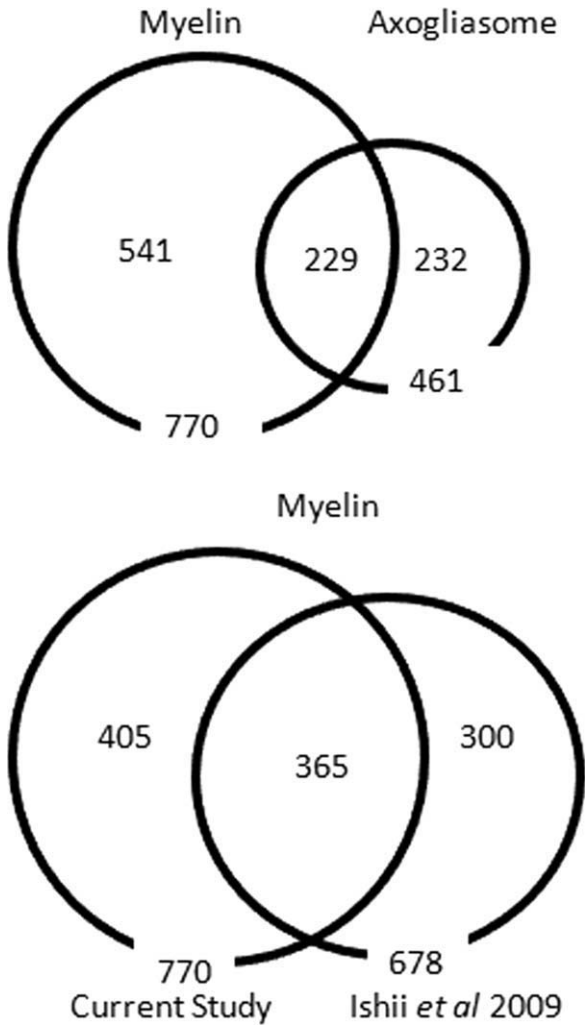

Fig. 3. The human axoglial specializations, myelin and axogliasomes, together are comprised of more than 1,000 proteins. (**A**) Venn diagram showing the overlap between myelin and axogliasomal fractions. A total of 770 and 461 proteins were identified in myelin and axogliasome fractions, respectively. Notably, 229 proteins were detectable in both axogliasomes and myelin. Unique and commonly identified proteins were classified according to molecular function (Supp. Info. Fig. 2) and are listed in Table 1. (**B**) We compared our proteome map to a recently generated human myelin proteome map (Ishii et al., 2009). We detected 370 myelin proteins that were also identified by Ishii et al. (2009).

Morales et al., 2009; Jahn et al., 2009; Kippert et al., 2008; Roth et al., 2006).

When comparing our human myelin proteome map to the proteome map generated by Ishii et al. (2009), we identified an overlap of 55% (Fig. 3 and Table 1). There are several factors that could contribute to the differences between the two studies. First, the material used in our study was from freshly excised tissue, whereas the material in Ishii et al. was obtained from postmortem subjects. This could have altered the composition and integrity of myelin. However, the overlap between the two studies suggests that myelin is relatively resistant to degradation for several hours. Second, the age of the subjects differed (20–45 years in our study vs. 53–65 years in Ishii et al.). In a recent study, the efficiency of remyelination in mice was shown to be regulated by age-dependent epigenetic control of gene expression (Shen et al., 2008). It is likely that myelin synthesis capability, integrity, and composition changes with the process of aging in humans as well. Finally, technical limitations of mass spectrometry may also contribute to difference as in other nonmyelin proteomics studies, very little overlap was found even when identical starting material was used (Chamrad and Meyer, 2005). Thus, degradation of the samples, the age of the subjects, and technical limitations could have contributed to the differences between the two studies.

Despite differences between studies, a reference library can be generated upon validating the overlapping proteins by immunohistochemistry (and/or *in situ* hybridization). Out of 678 proteins identified by Ishii et al. about 370 proteins were also detectable in our proteome map, suggesting that the commonly identified proteins could be genuine myelin proteins (see Fig. 3). We identified about 770 proteins in our screen, which includes about 400 potentially novel myelin components in humans. Importantly, the myelin proteome map generated here has expanded the current myelin proteome to more than 1,000 proteins. Whether the differences between the studies are due to the quality of the samples or due to technical limitations of mass spectroscopy cannot be stated at this stage. The high overlap between the studies suggests that myelin membranes are low in complexity when compared with whole brain homogenate or cell culture lysates. The high overlap also suggests that shotgun analysis of myelin membranes isolated by sequential sucrose gradient centrifugation (Norton and Poduslo, 1973) yields reproducible proteome maps.

Next we questioned if the human myelin proteome is different from the axoglial apparatus proteome. For this we compared the above proteome to the axoglial proteome (see Fig. 3). There is no other study that has examined the axoglial apparatus in humans. In our previous report, we identified OMGP as a component of node of Ranvier along with 45 other relevant proteins that are known components of the axoglial apparatus (Huang et al., 2005). Altogether, we identified over 450 proteins in the axoglial apparatus (Supp. Info. Table 1). When comparing the axoglial proteome to the myelin proteome, about 229 myelin proteins were also detected in axoglial fraction suggesting that the specializations have overlapping but distinct proteomes. In another study using rodent optic nerve as starting material, Ogawa and Rasband identified about 400 proteins in the axoglial apparatus (Ogawa and Rasband, 2009). Even though a faithful comparison between the two studies is not possible because of the different methodology used for the isolation of the fractions, the different starting material (species), and the different analysis platforms, we mapped the Uniprot ID of all our human proteins and compared the two axoglial fractions. To our surprise, we identified about 28% overlap between the studies (data not shown). This demonstrates a conservation of the axoglial apparatus and function of these proteins across different species. Among the proteins identified in the axogliasomal fraction, many are known to localize to the axoglial apparatus *in situ*. These include ANKYRIN2, ANKYRIN3, BAND4.1,

TABLE 1. Proteins Commonly Identified in Human Myelin and Axoglial Apparatus Fraction

SwissProt ID	Protein ID	Protein name	Gene name
P61604	CH10_HUMAN	10 kDa heat shock protein, mitochondrial (Hsp10)	HSPE1
P31946	1433B_HUMAN	14-3-3 protein beta/alpha (Protein kinase C inhibitor protein 1)	YWHAB
P62258	1433E_HUMAN	14-3-3 protein epsilon (14-3-3E)	YWHAE
Q04917	1433F_HUMAN	14-3-3 protein eta (Protein AS1)	YWHAH
P27348	1433T_HUMAN	14-3-3 protein theta (14-3-3 protein tau) (14-3-3 protein T-cell)	YWHAQ
P62847	RS24_HUMAN	40S ribosomal protein S24	RPS24
P26373	RL13_HUMAN	60S ribosomal protein L13 (Breast basic conserved protein 1)	RPL13
P62917	RL8_HUMAN	60S ribosomal protein L8	RPL8
Q01813	K6PP_HUMAN	6-phosphofructokinase type C (EC 2.7.1.11) (Phosphofructokinase 1)	PFKP
P24752	THIL_HUMAN	Acetyl-CoA acetyltransferase, mitochondrial (EC 2.3.1.9)	ACAT1
Q99798	ACON_HUMAN	Aconitate hydratase, mitochondrial (Aconitase)	ACO2
P68032	ACTC_HUMAN	Actin, alpha cardiac muscle 1 (Alpha-cardiac actin)	ACTC1
O95433	AHSA1_HUMAN	Activator of 90 kDa heat shock protein ATPase homolog 1	AHSA1
O14561	ACPM_HUMAN	Acyl carrier protein, mitochondrial (ACP)	NDUFAB1
P14621	ACYP2_HUMAN	Acylphosphatase-2 (EC 3.6.1.7) (Acylphosphate phosphohydrolase 2)	ACYP2
Q02952	AKA12_HUMAN	A-kinase anchor protein 12 (A-kinase anchor protein 250 kDa)	AKAP12
P49588	SYAC_HUMAN	Alanyl-tRNA synthetase, cytoplasmic (EC 6.1.1.7) (Alanine–tRNA ligase)	AARS
P35611	ADDA_HUMAN	Alpha-adducin (Erythrocyte adducin subunit alpha)	ADD1
P06733	ENOA_HUMAN	Alpha-enolase (EC 4.2.1.11) (2-phospho-D-glycerate hydro-lyase)	ENO1
Q16352	AINX_HUMAN	Alpha-internexin (Alpha-Inx) (66 kDa neurofilament protein)	INA
P27338	AOFB_HUMAN	Amine oxidase [flavin-containing] B (EC 1.4.3.4)	MAOB
Q01484	ANK2_HUMAN	Ankyrin-2 (Brain ankyrin) (Ankyrin-B) (Non-erythroid ankyrin)	ANK2
P04083	ANXA1_HUMAN	Annexin A1 (Annexin-1) (Annexin I) (Lipocortin I)	ANXA1
P25705	ATPA_HUMAN	ATP synthase subunit alpha, mitochondrial	ATP5A1
O75947	ATP5H_HUMAN	ATP synthase subunit d, mitochondrial	ATP5H
P30049	ATPD_HUMAN	ATP synthase subunit delta, mitochondrial (F-ATPase delta subunit)	ATP5D
P56385	ATP5I_HUMAN	ATP synthase subunit e, mitochondrial	ATP5I
P48047	ATPO_HUMAN	ATP synthase subunit O, mitochondrial (Oligomycin sensitivity conferral protein)	ATP5O
Q9UQB8	BAIP2_HUMAN	Brain-specific angiogenesis inhibitor 1-associated protein 2	BAIAP2
Q96GW7	PGCB_HUMAN	Brevican core protein (Brain-enriched hyaluronan-binding protein)	BCAN
Q13557	KCC2D_HUMAN	Calcium/calmodulin-dependent protein kinase type II delta chain	CAMK2D
B4DJ51	B4DJ51_HUMAN	Calmodulin 1 (Phosphorylase kinase, delta), isoform CRA_a	CALM1
P27824	CALX_HUMAN	Calnexin (Major histocompatibility complex class I antigen-binding protein p88)	CANX
P27797	CALR_HUMAN	Calreticulin (CRP55) (Calregulin) (HACBP) (ERp60) (grp60)	CALR
Q9UDT6	CLIP2_HUMAN	CAP-Gly domain-containing linker protein 2 (Cytoplasmic linker protein 2)	CLIP2
P16152	CBR1_HUMAN	Carbonyl reductase [NADPH] 1 (NADPH-dependent carbonyl reductase 1)	CBR1
P26232	CTNA2_HUMAN	Catenin alpha-2 (Alpha-catenin-related protein) (Alpha N-catenin)	CTNNA2
P07339	CATD_HUMAN	Cathepsin D [Cleaved into: Cathepsin D light chain; Cathepsin D heavy chain]	CTSD
Q9Y696	CLIC4_HUMAN	Chloride intracellular channel protein 4	CLIC4
Q00610	CLH1_HUMAN	Clathrin heavy chain 1 (CLH-17)	CLTC
P23528	COF1_HUMAN	Cofilin-1 (Cofilin, non-muscle isoform) (18 kDa phosphoprotein) (p18)	CFL1
Q9Y281	COF2_HUMAN	Cofilin-2 (Cofilin, muscle isoform)	CFL2
Q07021	C1QBP_HUMAN	Complement component 1 Q subcomponent-binding protein, mitochondrial	C1QBP
P78357	CNTP1_HUMAN	Contactin-associated protein 1 (Caspr1) (Caspr) (Neurexin 4) (Neurexin IV) (p190)	CNTNAP1
P12277	KCRB_HUMAN	Creatine kinase B-type (EC 2.7.3.2) (Creatine kinase B chain) (B-CK)	CKB
P46109	CRKL_HUMAN	Crk-like protein	CRKL
P04080	CYTB_HUMAN	Cystatin-B (Stefin-B) (Liver thiol proteinase inhibitor) (CPI-B)	CSTB
P21291	CSRP1_HUMAN	Cysteine and glycine-rich protein 1 (Cysteine-rich protein 1) (CRP1) (CRP)	CSRP1
P07919	QCR6_HUMAN	Cytochrome b-c1 complex subunit 6, mitochondrial	UQCRH
P20674	COX5A_HUMAN	Cytochrome c oxidase subunit 5A, mitochondrial	COX5A
P10606	COX5B_HUMAN	Cytochrome c oxidase subunit 5B, mitochondrial (Cytochrome c oxidase polypep. Vb)	COX5B
O43237	DC1L2_HUMAN	Cytoplasmic dynein 1 light intermediate chain 2	DYNC1LI2
Q96KP4	CNDP2_HUMAN	Cytosolic non-specific dipeptidase (CNDP dipeptidase 2)	CNDP2
O43175	SERA_HUMAN	D-3-phosphoglycerate dehydrogenase (3-PGDH) (EC 1.1.1.95)	PHGDH
Q14194	DPYL1_HUMAN	Dihydropyrimidinase-related protein 1 (DRP-1)	CRMP1
P31689	DNJA1_HUMAN	DnaJ homolog subfamily A member 1 (Heat shock 40 kDa protein 4)	DNAJA1
Q14203	DCTN1_HUMAN	Dynactin subunit 1 (150 kDa dynein-associated polypeptide)	DCTN1
Q05193	DYN1_HUMAN	Dynamin-1 (EC 3.6.5.5)	DNM1
Q9NP97	DLRB1_HUMAN	Dynein light chain roadblock-type 1 (Dynein light chain 2A, cytoplasmic)	DYNLRB1
P68104	EF1A1_HUMAN	Elongation factor 1-alpha 1 (EF-1-alpha-1) (Elongation factor 1 A-1)	EEF1A1
P13639	EF2_HUMAN	Elongation factor 2 (EF-2)	EEF2
P49411	EFTU_HUMAN	Elongation factor Tu, mitochondrial (EF-Tu) (P43)	TUFM
P14625	ENPL_HUMAN	Endoplasmin (Heat shock protein 90 kDa beta member 1)	HSP90B1
P30042	ES1_HUMAN	ES1 protein homolog, mitochondrial (Protein KNP-I) (Protein GT335)	C21orf33
P63241	IF5A1_HUMAN	Eukaryotic translation initiation factor 5A-1 (eIF-5A-1) (eIF-5A1)	EIF5A
P52907	CAZA1_HUMAN	F-actin-capping protein subunit alpha-1 (CapZ alpha-1)	CAPZA1
Q16658	FSCN1_HUMAN	Fascin (Singed-like protein) (55 kDa actin-bundling protein) (p55)	FSCN1
P04075	ALDOA_HUMAN	Fructose-bisphosphate aldolase A (EC 4.1.2.13) (Muscle-type aldolase)	ALDOA
P09972	ALDOC_HUMAN	Fructose-bisphosphate aldolase C (EC 4.1.2.13) (Brain-type aldolase)	ALDOC
P17931	LEG3_HUMAN	Galectin-3 (Galactose-specific lectin 3) (Mac-2 antigen) (IgE-binding protein)	LGALS3
Q9UEY8	ADDG_HUMAN	Gamma-adducin (Adducin-like protein 70)	ADD3
P09104	ENOG_HUMAN	Gamma-enolase (EC 4.2.1.11) (2-phospho-D-glycerate hydro-lyase)	ENO2
Q99747	SNAG_HUMAN	Gamma-soluble NSF attachment protein (SNAP-gamma)	NAPG
P06396	GELS_HUMAN	Gelsolin (Actin-depolymerizing factor) (ADF) (Brevin) (AGEL)	GSN
P14136	GFAP_HUMAN	Glial fibrillary acidic protein (GFAP)	GFAP
P00367	DHE3_HUMAN	Glutamate dehydrogenase 1, mitochondrial (GDH) (EC 1.4.1.3)	GLUD1
P15104	GLNA_HUMAN	Glutamine synthetase (GS) (EC 6.3.1.2) (Glutamate--ammonia ligase)	GLUL

TABLE 1. (Continued)

SwissProt ID	Protein ID	Protein name	Gene name
P04406	G3P_HUMAN	Glyceraldehyde-3-phosphate dehydrogenase (GAPDH) (EC 1.2.1.12)	GAPDH
Q9H4G4	GAPR1_HUMAN	Golgi-associated plant pathogenesis-related protein 1	GLIPR2
P62873	GBB1_HUMAN	Guanine nucleotide-binding protein G(I)/G(S)/G(T) subunit beta-1	GNB1
P09471	GNAO_HUMAN	Guanine nucleotide-binding protein G(o) subunit alpha	GNAO1
P08107	HSP71_HUMAN	Heat shock 70 kDa protein 1 (HSP70.1) (HSP70-1/HSP70-2)	HSPA1A
P11142	HSP7C_HUMAN	Heat shock cognate 71 kDa protein (Heat shock 70 kDa protein 8)	HSPA8
P04792	HSPB1_HUMAN	Heat shock protein beta-1 (HspB1) (Heat shock 27 kDa protein) (HSP 27)	HSPB1
P07900	HS90A_HUMAN	Heat shock protein HSP 90-alpha (HSP 86) (Renal carcinoma antigen NY-REN-38)	HSP90AA1
P54652	HSP72_HUMAN	Heat shock-related 70 kDa protein 2 (Heat shock 70 kDa protein 2)	HSPA2
P69905	HBA_HUMAN	Hemoglobin subunit alpha (Hemoglobin alpha chain) (Alpha-globin)	HBA1;HBA2
P68871	HBB_HUMAN	Hemoglobin subunit beta (Hemoglobin beta chain) (Beta-globin)	HBB
P05230	FGF1_HUMAN	Heparin-binding growth factor 1 (HBGF-1) (Acidic fibroblast growth factor)	FGF1
P61978	HNRPK_HUMAN	Heterogeneous nuclear ribonucleoprotein K (hnRNP K)	HNRNPK
P49773	HINT1_HUMAN	Histidine triad nucleotide-binding protein 1	HINT1
P04908	H2A1B_HUMAN	Histone H2A type 1-B/E (H2A/m) (H2A.2) (H2A/a)	HIST1H2AB
P20671	H2A1D_HUMAN	Histone H2A type 1-D (H2A.3) (H2A/g)	HIST1H2AD
P23527	H2B1O_HUMAN	Histone H2B type 1-O (H2B.n) (H2B/n) (H2B.2)	HIST1H2BO
P68431	H31_HUMAN	Histone H3.1 (H3/a) (H3/b) (H3/c) (H3/d) (H3/f) (H3/h) (H3/i) (H3/j) (H3/k) (H3/l)	HIST1H3A
P62805	H4_HUMAN	Histone H4	HIST1H4A
P48735	IDHP_HUMAN	Isocitrate dehydrogenase [NADP], mitochondrial (IDH)	IDH2
P04264	K2C1_HUMAN	Keratin, type II cytoskeletal 1 (Cytokeratin-1) (CK-1)	KRT1
P35908	K22E_HUMAN	Keratin, type II cytoskeletal 2 epidermal (Cytokeratin-2e)	KRT2
P14174	MIF_HUMAN	Macrophage migration inhibitory factor (MIF) (EC 5.3.2.1)	MIF
P40926	MDHM_HUMAN	Malate dehydrogenase, mitochondrial (EC 1.1.1.37)	MDH2
Q9H9H5	MA6D1_HUMAN	MAP6 domain-containing protein 1 (21 kDa STOP-like protein)	MAP6D1
P78559	MAP1A_HUMAN	Microtubule-associated protein 1A (MAP-1A)	MAP1A
P11137	MAP2_HUMAN	Microtubule-associated protein 2 (MAP-2)	MAP2
P27816	MAP4_HUMAN	Microtubule-associated protein 4 (MAP-4)	MAP4
Q15555	MARE2_HUMAN	Microtubule-associated protein RP/EB family member 2	MAPRE2
P10636	TAU_HUMAN	Microtubule-associated protein tau	MAPT (
O94826	TOM70_HUMAN	Mitochondrial import receptor subunit TOM70	TOMM70A
Q16891	IMMT_HUMAN	Mitochondrial inner membrane protein (Mitofilin)	IMMT
O00499	BIN1_HUMAN	Myc box-dependent-interacting protein 1	BIN1
P02686	MBP_HUMAN	Myelin basic protein, isoform 4	MBP
P60660	MYL6_HUMAN	Myosin light polypeptide 6 (Smooth muscle and nonmuscle myosin LC alkali 6)	MYL6
P19105	ML12A_HUMAN	Myosin regulatory light chain 12A (Myosin regulatory light chain MRLC3)	MYL12A
P35579	MYH9_HUMAN	Myosin-9 (Myosin heavy chain 9) (Myosin heavy chain, non-muscle IIa)	MYH9
P29966	MARCS_HUMAN	Myristoylated alanine-rich C-kinase substrate (MARCKS)	MARCKS
O94760	DDAH1_HUMAN	N(G),N(G)-dimethylarginine dimethylaminohydrolase 1	DDAH1
Q16718	NDUA5_HUMAN	NADH dehydrogenase [ubiquinone] 1 alpha subcomplex subunit 5	NDUFA5
P51970	NDUA8_HUMAN	NADH dehydrogenase [ubiquinone] 1 alpha subcomplex subunit 8	NDUFA8
O96000	NDUBA_HUMAN	NADH dehydrogenase [ubiquinone] 1 beta subcomplex subunit 10	NDUFB10
Q4QRK6	Q4QRK6_HUMAN	NEFM protein (Neurofilament 3 (150kDa medium))	NEFM
P61601	NCALD_HUMAN	Neurocalcin-delta	NCALD
P12036	NFH_HUMAN	Neurofilament heavy polypeptide (NF-H)	NEFH
P07196	NFL_HUMAN	Neurofilament light polypeptide (NF-L)	NEFL
Q9UH03	SEPT3_HUMAN	Neuronal-specific septin-3	SEPT3
P55209	NP1L1_HUMAN	Nucleosome assembly protein 1-like 1 (NAP-1-related protein)	NAP1L1
Q99733	NP1L4_HUMAN	Nucleosome assembly protein 1-like 4 (Nucleosome assembly protein 2) (NAP2)	NAP1L4
Q9NTK5	OLA1_HUMAN	Obg-like ATPase 1 (EC 3.6.3.-) (GTP-binding protein 9)	OLA1
P62937	PPIA_HUMAN	Peptidyl-prolyl *cis-trans* isomerase A (PPIase A)	PPIA
P23284	PPIB_HUMAN	Peptidyl-prolyl *cis-trans* isomerase B (PPIase)	PPIB
Q06830	PRDX1_HUMAN	Peroxiredoxin-1 (EC 1.11.1.15) (Thioredoxin peroxidase 2)	PRDX1
P32119	PRDX2_HUMAN	Peroxiredoxin-2 (EC 1.11.1.15) (Thioredoxin peroxidase 1)	PRDX2
P30044	PRDX5_HUMAN	Peroxiredoxin-5, mitochondrial (EC 1.11.1.15) (Prx-V)	PRDX5
P30086	PEBP1_HUMAN	Phosphatidylethanolamine-binding protein 1 (PEBP-1)	PEBP1
P00558	PGK1_HUMAN	Phosphoglycerate kinase 1 (EC 2.7.2.3) (Primer recognition protein 2)	PGK1
P36969	GPX4_HUMAN	Phospholipid hydroperoxide glutathione peroxidase, mitochondrial	GPX4
Q15149	PLEC1_HUMAN	Plectin-1 (PLTN) (PCN) (Hemidesmosomal protein 1)	PLEC1
Q15365	PCBP1_HUMAN	Poly(rC)-binding protein 1 (Alpha-CP1) (hnRNP-E1) (NA-binding protein SUB2.3)	PCBP1
P07737	PROF1_HUMAN	Profilin-1 (Profilin I)	PFN1
P35080	PROF2_HUMAN	Profilin-2 (Profilin II)	PFN2
P35232	PHB_HUMAN	Prohibitin	PHB
P30101	PDIA3_HUMAN	Protein disulfide-isomerase A3 (EC 5.3.4.1) (Disulfide isomerase ER-60)	PDIA3
Q7L099	RUFY3_HUMAN	Protein RUFY3 (Rap2-interacting protein x) (RIPx)	RUFY3
P04271	S100B_HUMAN	Protein S100-B (S100 calcium-binding protein B)	S100B
P22061	PIMT_HUMAN	Protein-L-isoaspartate(D-aspartate) *O*-methyltransferase	PCMT1
O75061	AUXI_HUMAN	Putative tyrosine-protein phosphatase auxilin (EC 3.1.3.48)	DNAJC6
P11177	ODPB_HUMAN	Pyruvate dehydrogenase E1 component subunit beta, mitochondrial	PDHB
P14618	KPYM_HUMAN	Pyruvate kinase isozymes M1/M2 (EC 2.7.1.40) (Pyruvate kinase muscle isozyme)	PKM2
P31150	GDIA_HUMAN	Rab GDP dissociation inhibitor alpha (Rab GDI alpha)	GDI1
P43487	RANG_HUMAN	Ran-specific GTPase-activating protein (Ran-binding protein 1)	RANBP1
P61026	RAB10_HUMAN	Ras-related protein Rab-10	RAB10
Q16799	RTN1_HUMAN	Reticulon-1 (Neuroendocrine-specific protein)	RTN1 (NSP)
O95197	RTN3_HUMAN	Reticulon-3 (Neuroendocrine-specific protein-like 2)	RTN3
P52565	GDIR1_HUMAN	Rho GDP-dissociation inhibitor 1 (Rho GDI 1) (Rho-GDI alpha)	ARHGDIA
Q7L7Q5	Q7L7Q5_HUMAN	RTN4 isoform C (RTN4) (Reticulon 4, isoform CRA_d)	RTN4
Q12765	SCRN1_HUMAN	Secernin-1	SCRN1

TABLE 1. (Continued)

SwissProt ID	Protein ID	Protein name	Gene name
Q9NVA2	SEP11_HUMAN	Septin-11	SEP11
Q15019	SEPT2_HUMAN	Septin-2 (Neural precursor cell expressed developmentally down-regulated protein 5)	SEPT2
O43236	SEPT4_HUMAN	Septin-4 (Peanut-like protein 2) (Brain protein H5) (CDC-related protein 2)	SEPT4
Q16181	SEPT7_HUMAN	Septin-7 (CDC10 protein homolog)	SEPT7
O15075	DCLK1_HUMAN	Serine/threonine-protein kinase DCLK1	DCLK1
P02787	TRFE_HUMAN	Serotransferrin (Transferrin) (Siderophilin) (Beta-1 metal-binding globulin)	TF
P05026	AT1B1_HUMAN	Sodium/potassium-transporting ATPase subunit beta-1, isoform 2	ATP1B1
O60493	SNX3_HUMAN	Sorting nexin-3 (Protein SDP3)	SNX3
Q13813	SPTA2_HUMAN	Spectrin alpha chain, brain (Spectrin, non-erythroid alpha chain) (Alpha-II spectrin)	SPTAN1
Q01082	SPTB2_HUMAN	Spectrin beta chain, brain 1 (Spectrin, non-erythroid beta chain 1) (Beta-II spectrin)	SPTBN1
P38646	GRP75_HUMAN	Stress-70 protein, mitochondrial (75 kDa glucose-regulated protein) (GRP 75)	HSPA9
P31948	STIP1_HUMAN	Stress-induced-phosphoprotein 1 (STI1) (Hsc70/Hsp90-organizing protein)	STIP1
P17600	SYN1_HUMAN	Synapsin-1 (Synapsin I) (Brain protein 4.1)	SYN1
Q92777	SYN2_HUMAN	Synapsin-2 (Synapsin II)	SYN2
P60880	SNP25_HUMAN	Synaptosomal-associated protein 25	SNAP25
P61764	STXB1_HUMAN	Syntaxin-binding protein 1 (Unc-18 homolog)	STXBP1
Q9UDY2	ZO2_HUMAN	Tight junction protein ZO-2 (Zonula occludens protein 2)	TJP2
P40939	ECHA_HUMAN	Trifunctional enzyme subunit alpha, mitochondrial (TP-alpha)	HADHA
P60174	TPIS_HUMAN	Triosephosphate isomerase (TIM)	TPI1
O14773	TPP1_HUMAN	Tripeptidyl-peptidase 1 (TPP-1) (EC 3.4.14.9)	TPP1
Q9NZR1	TMOD2_HUMAN	Tropomodulin-2 (Neuronal tropomodulin)	TMOD2
P04350	TBB4_HUMAN	Tubulin beta-4 chain (Tubulin 5 beta)	TUBB4
O94811	TPPP_HUMAN	Tubulin polymerization-promoting protein (TPPP)	TPPP
Q9UHD9	UBQL2_HUMAN	Ubiquilin-2 (Protein linking IAP with cytoskeleton 2)	UBQLN2
Q3MIH3	Q3MIH3_HUMAN	Ubiquitin A-52 residue ribosomal protein fusion product 1	UBA52
P09936	UCHL1_HUMAN	Ubiquitin carboxyl-terminal hydrolase isozyme L1 (UCH-L1)	UCHL1
P61088	UBE2N_HUMAN	Ubiquitin-conjugating enzyme E2 N (EC 6.3.2.19)	UBE2N
Q9H425	CA198_HUMAN	Uncharacterized protein C1orf198	C1orf198
P46459	NSF_HUMAN	Vesicle-fusing ATPase (EC 3.6.4.6) (*N*-ethylmaleimide-sensitive fusion protein)	NSF
P08670	VIME_HUMAN	Vimentin	VIM
P21796	VDAC1_HUMAN	Voltage-dependent anion-selective channel protein 1 (VDAC-1) (hVDAC1)	VDAC1
Q9Y277	VDAC3_HUMAN	Voltage-dependent anion-selective channel protein 3 (VDAC-3) (hVDAC3)	VDAC3
P21281	VATB2_HUMAN	V-type proton ATPase subunit B, brain isoform (V-ATPase subunit B 2)	ATP6V1B2
P61421	VA0D1_HUMAN	V-type proton ATPase subunit d 1 (V-ATPase subunit d 1)	ATP6V0D1
P36543	VATE1_HUMAN	V-type proton ATPase subunit E 1 (V-ATPase subunit E 1)	ATP6V1E1
Q16864	VATF_HUMAN	V-type proton ATPase subunit F (V-ATPase subunit F)	ATP6V1F
Protiens reported in our previous study (Huang et al., 2005)			
O75077	ADA23_HUMAN	Disintegrin and metalloproteinase domain-containing protein 23 (ADAM 23)	ADAM23
Q13740	CD166_HUMAN	CD166 antigen (Activated leukocyte cell adhesion molecule)	ALCAM
Q12955	ANK3_HUMAN	Ankyrin-3 (ANK-3) (Ankyrin-G)	ANK3
P54707	AT12A_HUMAN	Potassium-transporting ATPase alpha chain 2 (EC 3.6.3.10)	ATP12A
P50993	AT1A2_HUMAN	Sodium/potassium-transporting ATPase subunit alpha-2	ATP1A2
Q13733	AT1A4_HUMAN	Sodium/potassium-transporting ATPase subunit alpha-4	ATP1A4
P14415	AT1B2_HUMAN	Sodium/potassium-transporting ATPase subunit beta-2	ATP1B2
P35613	BASI_HUMAN	Basigin (Leukocyte activation antigen M6) (Collagenase stimulatory factor)	BSG
P10909	CLUS_HUMAN	Clusterin (Complement-associated protein SP-40,40)	CLU
P09543	CN37_HUMAN	2′,3′-cyclic-nucleotide 3′-phosphodiesterase (CNPase)	CNP
Q12860	CNTN1_HUMAN	Contactin-1 (Neural cell surface protein F3)	CNTN1
P02511	CRYAB_HUMAN	Alpha-crystallin B chain (Alpha(B)-crystallin)	CRYAB
Q9UJU6	DBNL_HUMAN	Drebrin-like protein (Drebrin-F) (SH3 domain-containing protein 7)	DBNL
Q16555	DPYL2_HUMAN	Dihydropyrimidinase-related protein 2 (DRP-2)	DPYSL2
Q14195	DPYL3_HUMAN	Dihydropyrimidinase-related protein 3 (DRP-3)	DPYSL3
O14531	DPYL4_HUMAN	Dihydropyrimidinase-related protein 4 (DRP-4)	DPYSL4
O43491	E41L2_HUMAN	Band 4.1-like protein 2 (Generally expressed protein 4.1)	EPB41L2
O75955	FLOT1_HUMAN	Flotillin-1	FLOT1
P06241	FYN_HUMAN	Tyrosine-protein kinase Fyn (EC 2.7.10.2) (Proto-oncogene c-Fyn) (p59-Fyn)	FYN
Q9UN86	G3BP2_HUMAN	Ras GTPase-activating protein-binding protein 2 (G3BP-2)	G3BP2
P50148	GNAQ_HUMAN	Guanine nucleotide-binding protein G(q) subunit alpha	GNAQ
P62879	GBB2_HUMAN	Guanine nucleotide-binding protein G(I)/G(S)/G(T) subunit beta-2	GNB2
Q969P0	IGSF8_HUMAN	Immunoglobulin superfamily member 8 (IgSF8) (CD81 partner 3)	IGSF8
P16389	KCNA2_HUMAN	Potassium voltage-gated channel subfamily A member 2	KCNA2
P20916	MAG_HUMAN	Myelin-associated glycoprotein (Siglec-4a)	MAG
P02686	MBP_HUMAN	Myelin basic protein (MBP) (Myelin A1 protein)	MBP
P13591	NCAM1_HUMAN	Neural cell adhesion molecule 1 (N-CAM-1)	NCAM1
O94856	NFASC_HUMAN	Neurofascin	NFASC
Q5VXU1	NKAI2_HUMAN	Sodium/potassium-transporting ATPase subunit beta-1-interacting protein 2	NKAIN2
P23515	OMGP_HUMAN	Oligodendrocyte-myelin glycoprotein, Oligodendrocyte-myelin glycoprotein	OMG
Q9Y342	PLLP_HUMAN	Plasmolipin (Plasma membrane proteolipid)	PLLP
P02689	MYP2_HUMAN	Myelin P2 protein	PMP2
Q01453	PMP22_HUMAN	Peripheral myelin protein 22 (PMP-22) (Growth arrest-specific protein 3)	PMP22
P17252	KPCA_HUMAN	Protein kinase C alpha type (PKC-alpha) (PKC-A)	PRKCA
Q99962	SH3G2_HUMAN	Endophilin-A1 (Endophilin-1) (SH3 domain-containing GRB2-like protein 2)	SH3GL2
P04216	THY1_HUMAN	Thy-1 membrane glycoprotein (Thy-1 antigen) (CDw90) (CD antigen CD90)	THY1
Q14106	TOB2_HUMAN	Protein Tob2 (Transducer of erbB-2 2) (Protein Tob4)	TOB2
P13611	CSPG2_HUMAN	Versican core protein (Large fibroblast proteoglycan)	VCAN

Proteins with more than two unique peptides were considered in this analysis, with exception to known myelin components (see Supp.Info. Table 2 for details about the number of peptides per protein), where a single peptide was considered sufficient for inclusion into the proteome map.

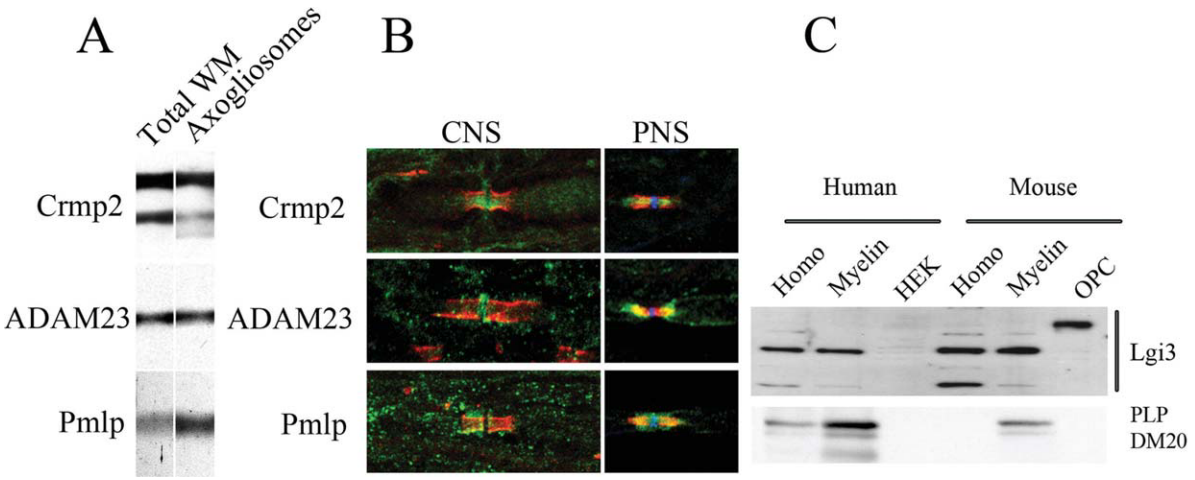

Fig. 4. MudPIT identified axogliasomal and myelin proteins are present in respective CNS and PNS compartments. (**A**) Crmp-2, Adam23, and plasmolipin are enriched in the axogliasomal fraction to different extents when compared with the HWM homogenate. The two major bands recognized by the CRMP-2 antibody correspond to the alternatively spliced longer and shorter isoforms. (**B**) Spinal cord or sciatic nerve sections from P18 rat were stained for Adam23, Crmp2, and plasmolipin (in green) and Caspr (in red) to label paranodes. The PNS sections were also labeled with pan-sodium channel antibody (in blue). (**C**) Immunoblotting of human white matter and mouse brain homogenate (Homo) and myelin for LGI3, identified in the myelin fraction, showing the major isoform (65 kDa), a smaller isoform (30 kDa), which may represent proteolytic cleavage. A higher molecular weight product, which may represent a glycosylated form, is present in a murine oligodendrocyte precursor cell line (oli-neu; OPC). Human embryonic kidney cells (HEK) cells express undetectable amounts of LGI3. The PLP/DM20 blot shows that the myelin fractions are enriched in compact myelin proteins.

ALPHA and BETA SPECTRIN, CLUSTERIN, ABDDUCIN, SEPTINS, CASPR, CONTACTIN1, CONTACTIN2, NEUREXIN, OMGP, VERSICAN, CNP, CRMPS, MAG, voltage-gated sodium, and potassium channels (Pedraza et al., 2001; Poliak and Peles, 2003; Salzer et al., 2008; Table 1 and Supp. Info. Table 1).

We further categorized each identified protein by its anticipated molecular function to determine whether we might assess myelin and axogliasomes as functional subcellular compartments (Supp. Info. Fig. 2). Using the Panther database classification system, we found proteins of diverse function including transfer/carrier proteins, ion channels, receptors, regulatory molecules, membrane trafficking proteins, signaling molecules, chaperones, cell junction protein, cell adhesion molecule, and kinases. The identification of these proteins suggests presence of biosynthesis/trafficking, protein folding, degradation, regulation and homeostasis organelles within paranodal loops.

Localization of MudPIT Identified Proteins at the Axoglial Apparatus and in Myelin

We used antibodies to four candidate proteins, a disintegrin and metalloprotease protein 23 (ADAM23), collapsin response mediator protein-2 (CRMP-2), plasmolipin and leucine-rich glioma-inactivated protein 3 (LGI3) to determine their presence at the respective axoglial specializations. All proteins except LGI3 were present in the MudPIT screen in both fractions. By Western blot analysis, we found ADAM23, CRMP-2, and plasmolipin were enriched in the axoglial specialization fraction to different extents when compared with HWM homogenate (Fig. 4A). Immunoblotting for LGI3 revealed that the major 65-kDa isoform of LGI3 is enriched in both human and murine myelin fractions when compared with whole brain homogenates (Fig. 4C). We next examined the distributions of these axoglial apparatus identified molecules by immunohistochemistry in CNS and PNS fibers.

The CRMP family consists of five cytosolic phosphoproteins (CRMP1-5), (Charrier et al., 2003; Schmidt and Strittmatter, 2007), each with short and long isoforms. Although, the functions of CRMPs have to date mostly been described in neurons (Inagaki et al., 2001; Kamata et al., 1998; Liu and Strittmatter, 2001), it is also known that CRMP-2 is present in oligodendrocytes (Ricard et al., 2000). All five CRMPs were identified in our screen (Table 1 and Supp. Info. Table 2). Because of the high homology between different CRMPs, most antibodies recognize all CRMP isoforms. Using an antibody directed against a CRMP-2 peptide (Ricard et al., 2000), we observed CRMPs to be localized in the axoplasm of the paranodal/nodal region in CNS and PNS fibers, rather than throughout the axon (see Fig. 4). In unmyelinated axons, CRMP-labeling is uniformly distributed throughout the axoplasm (Supp. Info. Fig. 2), suggesting that components from myelin may regulate CRMP distribution in the axon, similar to the regulated distribution of neurofilaments through myelin ensheathment (Brady et al., 1999). ADAM23 is a member of the disintegrin family that is highly expressed in the CNS (Lin et al., 2010; Sagane et al., 1999) and is known to modulate integrin signaling (Verbisck et al., 2009). Mutant mice lacking *Adam23* exhibit severe tremor and ataxia (Mitchell et al., 2001), suggesting perturbed myelination. Recently, another Adam family member, Adam22, was shown to bind to Lgi family proteins (Ozkaynak et al., 2010). Lgi4-null mice are hypomyelinated suggesting that Lgi-Adam signaling play a key role in myelination

(Bermingham et al., 2006). Immunohistochemistry revealed that Adam23 is distributed at the outermost paranodal membrane in both CNS and PNS fibers (Fig. 4 and Supp. Info. Fig. 2). In CNS fibers, outer paranodal membrane staining is detectable in large axonal processes, likely derived from motor neurons in the spinal cord. It is unclear why paranodal membranes in smaller axons are not labeled by Adam23 antibody. In PNS fibers, Adam23 strongly labeled paranodal membranes (see Fig. 4) as well as the outer mesaxon. In addition, Adam23 is also detected in Schmidt-Lanternmann incisures, cytoplasmic channels found within compact myelin of PNS fibers (Supp. Info. Fig. 2).

Plasmolipin is a tetraspan (4-TM) lipid-binding protein that is abundantly expressed in CNS and PNS myelin membranes, as well as apical tubular cells in the kidney (Fischer and Sapirstein, 1994). This molecule and other tetraspanins, such as proteolipid protein, PLP (Kitagawa et al., 1993), are proposed as potential pore-forming cation-specific ion channels upon oligomerization. In CNS and PNS fibers, we detected plasmolipin in the paranodal loops (see Fig. 4). As a putative lipid-binding protein (Fischer et al., 1994), plasmolipin may potentially play a role in the assembly and delivery of lipid-bound protein complexes, such lipid raft components, or mRNA transport granules to sites of axon–glia interaction at the paranodes. In fact, another myelin-specific protein also identified in our screen, MAL2, was demonstrated to play a role in transcytosis, a process of targeting protein components to the apical membrane surface (de Marco et al., 2002).

DISCUSSION

In this study, we have isolated and analyzed CNS white matter subfractions enriched in paranodal axoglial and myelin membranes. Axoglial junctions remain stably associated with axonal and glial membranes and retained septate densities at the axon-myelin cleft even under hyperosmotic treatment and detergent extractions, providing evidence that the axoglial junction is a *bona fide* adhesive zone formed between the neuron and the myelinating cell (Pedraza et al., 2001). Our proteomic analysis identified proteins of quite varied molecular and cellular functions including proteins and subunits required for metabolic machineries such as mitochondria, for lysosomal and endoplasmic reticulum protein/lipid biosynthesis, as well as degradation machinery proteins, chaperones, receptors, and structural, scaffolding, signaling, and cell adhesion molecules. Possible roles of molecules identified in the current screen are discussed below.

Classical Myelin and Axogliasomal Molecules

The quantitative predominance of classical myelin and paranodal proteins including PLP, MBP, and voltage-gated channels at respective specializations historically led to a conception that internodal and axoglial specializations are low in complexity. However, during the past decade and in the current study, several hundred molecules were identified in rodent and human myelin membranes and axogliasomal structures. In addition to classical proteins, we also identified several adhesion molecules, cytoskeletal, and scaffolding proteins that are differentially found in both axoglial specializations. This includes NECLS, CLAUDINS, CONTACTINS, CASPR, CAMS, DMS, EZRIN, ACTINS, ARP2/3, 14-3-3, ANKYRIN, and TUBULIN. In the rodent brain, contact-dependent and -independent clustering of voltage-gated sodium channels (NaV) at the node is triggered by paranodal axoglial junctions between glial nfasc155 and axonal caspr and contactin, which also coincides with the clustering of some of the nodal/paranodal components such as nfasc186, nrcam, ankyrin G (ankG), and βIV-spectrin (Kaplan et al., 1997; Pedraza et al., 2001; Poliak and Peles, 2003; Susuki and Rasband, 2008). Compact myelin has been shown to be required for clustering of Kv channels (Baba et al., 1999). Taken together, the engagement of complex neuron-to-glia interactions recruiting different molecules may act synchronously to establish discrete domains in myelinated fibers.

Endoplasmic Reticulum (ER), Soluble Chaperones, and Translational Machinery

The presence of ER-associated and soluble chaperones in these axoglial specializations indicates that local synthesis and folding of proteins may occur. Proteins including CALNEXIN, CALRETICULIN, PDIs, and soluble HSPs were found in both fractions. The axoglial apparatus distribution of ER-localized inositol 1,4,5-trisphosphate receptors (IP3Rs) and calnexin was recently reported (Toews et al., 2007). This peculiar distribution of calnexin, might explain the early postnatal death and motor disorders in mice congenitally deficient in calnexin (Denzel et al., 2002), which is also associated with a dramatic loss of large myelinated nerve fibers. Myelination per se appears normal in these null mice; however, it is possible that paranodal and nodal calnexin governs the glycosylation status or adhesion properties of adhesion molecules and ion channels. PLP has been shown to interact with calreticulin and integrins (Gudz et al., 2002), thus detection of calreticulin is also not surprising. The paranodal complex of F3/Contactin and Caspr/Paranodin has been shown to traffic to the cell surface via a nonconventional pathway, in which the intermediate Golgi is bypassed and the proteins are delivered directly to the cell surface (Bonnon et al., 2003), suggesting the presence of ER membranes in the axoglial apparatus.

The presence of protein translational machinery is neither new nor unique to such a structure. Local translation is also known to occur in axonal growth cones, presynaptic spines, and postsynaptic scaffolds (Holbro et al., 2009). Also, we have previously reported the translocation of *MBP* mRNA in myelin and local translation of MBP mRNAs in the myelin membrane (Boccaccio and Colman, 1995; Colman et al., 1982). In addition, two RNA binding proteins, hnRNPA2/B1 and quaking, were shown to trans-

port myelin basic protein (MBP) transcripts to myelinating membranes in the OL (Carson et al., 1998; Hardy, 1998; White et al., 2008). The presence of rough ER in the axoglial apparatus compartment would enable efficient responses to local metabolic demands.

Secretory Pathway Machinery and Regulators

In addition to newly synthesized proteins and lipids, the long-term integrity of nodal, paranodal, and internodal myelin membranes require recycling of receptors and structural components. This is dependent on efficient endocytic uptake, degradation compartments, SNARE machinery for regulating membrane flow, and small GTPases as regulators of key steps. Several RABs, SNAREs, proteosomal, endosomal, and lysosomal proteins were identified at both axoglial specializations indicating that the machinery required for these functions is present.

Other Proteins and Axon-to-Glial Interaction and Support

In addition to delivery and uptake of proteins at these sites, to and fro communication between axons and glia is also required for continuous glial support for neuronal survival. The uncoupling of glial support has been shown to dictate the health of myelinated nerves, since mice lacking oligodendroglial proteins plp1, cnpase, and pex5, are known to exhibit perturbed glial support, leading to axonal degeneration (Nave and Trapp, 2008). Signaling molecules, receptors, and downstream effectors implicated in such processes including FYN, CDCS, SEPTINS, ERBBS, small GTPASES, and other KINASES were detected in the current screen.

The protein composition of human myelin and the axoglial apparatus appears larger than previously anticipated. Several new proteins may also have copurified with myelin, for example mitochondrial proteins, due to trapping phenomena and the high sensitivity of the detection system. However, a recent report using *in vivo* imaging in the mouse of a mitochondrial-cox8 ECFP fusion protein revealed immobility of mitochondria at the node of Ranvier (Misgeld et al., 2007) and enrichment of mitochondrial oxidative complex protein in axogliasomes was reported previously (Roth et al., 2006). Thus the copurification of mitochondrial and ribosomal proteins may also be attributed to their relatively low mobility due to interaction with scaffolding molecules at axoglial regions. Interestingly, proteomic profiling of mammalian brain mitochondria and synaptic vesicles revealed the presence of classical myelin proteins such as PLP, MBP, MOBP, MAG, Nfscn, and Caspr (Pagliarini et al., 2008; Takamori et al., 2006).

Loss of normal myelin is an underlying cause of disability in various white matter diseases, including multiple sclerosis and a variety of leukodystrophies. During such CNS damage, the node of Ranvier is disrupted, impairing nerve conduction. Autoantigenicity to several abundant myelin proteins like PLP, MBP, MOG, MAG etc is known to occur in multiple sclerosis. Surprisingly, the auto-antigen properties of quantitatively minor proteins of the axoglial apparatus, including CONTACTIN2 and NFSCN were recently reported in patients with multiple sclerosis (Derfuss et al., 2009; Mathey et al., 2007). The possibility exist that several novel myelin and axogliasomal proteins identified in our screen might act as autoantigens or play a role in the etiology of multiple sclerosis. With the human myelin and axoglial proteome atlas presented here, the role of many previously unidentified components can be addressed in health and disease.

ACKNOWLEDGMENTS

The authors wish to thank M. Pool, S. Rajasekharan, R. McAdam, and D. Liazoghli for helpful discussions.

REFERENCES

Baba H, Akita H, Ishibashi T, Inoue Y, Nakahira K, Ikenaka K. 1999. Completion of myelin compaction, but not the attachment of oligodendroglial processes triggers K(+) channel clustering. J Neurosci Res 58:752–764.

Bello-Morales R, de Marco MC, Aranda JF, Matesanz F, Alcina A, Lopez-Guerrero JA. 2009. Characterization of the MAL2-positive compartment in oligodendrocytes. Exp Cell Res 315:3453–3465.

Bermingham JR Jr, Shearin H, Pennington J, O'Moore J, Jaegle M, Driegen S, van Zon A, Darbas A, Ozkaynak E, Ryu EJ, Milbrandt J, Meijer D. 2006. The claw paw mutation reveals a role for Lgi4 in peripheral nerve development. Nat Neurosci 9:76–84.

Bernier L, Alvarez F, Norgard EM, Raible DW, Mentaberry A, Schembri JG, Sabatini DD, Colman DR. 1987. Molecular cloning of a 2′,3′-cyclic nucleotide 3′-phosphodiesterase: mRNAs with different 5′ ends encode the same set of proteins in nervous and lymphoid tissues. J Neurosci 7:2703–2710.

Boccaccio GL, Colman DR. 1995. Myelin basic protein mRNA localization and polypeptide targeting. J Neurosci Res 42:277–286.

Bonnon C, Goutebroze L, Denisenko-Nehrbass N, Girault JA, Faivre-Sarrailh C. 2003. The paranodal complex of F3/contactin and caspr/paranodin traffics to the cell surface via a non-conventional pathway. J Biol Chem 278:48339–48347.

Brady ST, Witt AS, Kirkpatrick LL, de Waegh SM, Readhead C, Tu PH, Lee VM. 1999. Formation of compact myelin is required for maturation of the axonal cytoskeleton. J Neurosci 19:7278–7288.

Cahoy JD, Emery B, Kaushal A, Foo LC, Zamanian JL, Christopherson KS, Xing Y, Lubischer JL, Krieg PA, Krupenko SA, Thompson WJ, Barres BA. 2008. A transcriptome database for astrocytes, neurons, and oligodendrocytes: A new resource for understanding brain development and function. J Neurosci 28:264–278.

Carson JH, Kwon S, Barbarese E. 1998. RNA trafficking in myelinating cells. Curr Opin Neurobiol 8:607–612.

Chamrad D, Meyer HE. 2005. Valid data from large-scale proteomics studies. Nat Methods 2:647–648.

Charrier E, Reibel S, Rogemond V, Aguera M, Thomasset N, Honnorat J. 2003. Collapsin response mediator proteins (CRMPs): Involvement in nervous system development and adult neurodegenerative disorders. Mol Neurobiol 28:51–64.

Colman DR, Kreibich G, Frey AB, Sabatini DD. 1982. Synthesis and incorporation of myelin polypeptides into CNS myelin. J Cell Biol 95(2, Part 1):598–608.

de Marco MC, Martin-Belmonte F, Kremer L, Albar JP, Correas I, Vaerman JP, Marazuela M, Byrne JA, Alonso MA. 2002. MAL2, a novel raft protein of the MAL family, is an essential component of the machinery for transcytosis in hepatoma HepG2 cells. J Cell Biol 159:37–44.

Denzel A, Molinari M, Trigueros C, Martin JE, Velmurgan S, Brown S, Stamp G, Owen MJ. 2002. Early postnatal death and motor disorders in mice congenitally deficient in calnexin expression. Mol Cell Biol 22:7398–7404.

Derfuss T, Parikh K, Velhin S, Braun M, Mathey E, Krumbholz M, Kumpfel T, Moldenhauer A, Rader C, Sonderegger P, Pollmann W, Tiefenthaller C, Bauer J, Lassmann H, Wekerle H, Karagogeos D, Hohlfeld R, Linington C, Meinl E. 2009. Contactin-2/TAG-1-directed

autoimmunity is identified in multiple sclerosis patients and mediates gray matter pathology in animals. Proc Natl Acad Sci USA 106:8302–8307.
Dhaunchak AS, Nave KA. 2007. A common mechanism of PLP/DM20 misfolding causes cysteine-mediated endoplasmic reticulum retention in oligodendrocytes and Pelizaeus-Merzbacher disease. Proc Natl Acad Sci USA 104:17813–17818.
Dugas JC, Tai YC, Speed TP, Ngai J, Barres BA. 2006. Functional genomic analysis of oligodendrocyte differentiation. J Neurosci 26:10967–10983.
Fischer I, Durrie R, Sapirstein VS. 1994. Plasmolipin: The other myelin proteolipid. A review of studies on its structure, expression, and function. Neurochem Res 19:959–966.
Fischer I, Sapirstein VS. 1994. Molecular cloning of plasmolipin. Characterization of a novel proteolipid restricted to brain and kidney. J Biol Chem 269:24912–24919.
Gudz TI, Schneider TE, Haas TA, Macklin WB. 2002. Myelin proteolipid protein forms a complex with integrins and may participate in integrin receptor signaling in oligodendrocytes. J Neurosci 22:7398–7407.
Hardy RJ. 1998. Molecular defects in the dysmyelinating mutant quaking. J Neurosci Res 51:417–422.
Holbro N, Grunditz A, Oertner TG. 2009. Differential distribution of endoplasmic reticulum controls metabotropic signaling and plasticity at hippocampal synapses. Proc Natl Acad Sci USA 106:15055–15060.
Huang JK, Phillips GR, Roth AD, Pedraza L, Shan W, Belkaid W, Mi S, Fex-Svenningsen A, Florens L, Yates JR III, Colman DR. 2005. Glial membranes at the node of Ranvier prevent neurite outgrowth. Science 310:1813–1817.
Inagaki N, Chihara K, Arimura N, Menager C, Kawano Y, Matsuo N, Nishimura T, Amano M, Kaibuchi K. 2001. CRMP-2 induces axons in cultured hippocampal neurons. Nat Neurosci 4:781–782.
Ishii A, Dutta R, Wark GM, Hwang SI, Han DK, Trapp BD, Pfeiffer SE, Bansal R. 2009. Human myelin proteome and comparative analysis with mouse myelin. Proc Natl Acad Sci USA 106:14605–14610.
Jahn O, Tenzer S, Werner HB. 2009. Myelin proteomics: Molecular anatomy of an insulating sheath. Mol Neurobiol 40:55–72.
Kamata T, Subleski M, Hara Y, Yuhki N, Kung H, Copeland NG, Jenkins NA, Yoshimura T, Modi W, Copeland TD. 1998. Isolation and characterization of a bovine neural specific protein (CRMP-2) cDNA homologous to unc-33, a *C. elegans* gene implicated in axonal outgrowth and guidance. Brain Res Mol Brain Res 54:219–236.
Kaplan MR, Meyer-Franke A, Lambert S, Bennett V, Duncan ID, Levinson SR, Barres BA. 1997. Induction of sodium channel clustering by oligodendrocytes. Nature 386:724–728.
Kippert A, Trajkovic K, Fitzner D, Opitz L, Simons M. 2008. Identification of Tmem10/Opalin as a novel marker for oligodendrocytes using gene expression profiling. BMC Neurosci 9:40.
Kitagawa K, Sinoway MP, Yang C, Gould RM, Colman DR. 1993. A proteolipid protein gene family: Expression in sharks and rays and possible evolution from an ancestral gene encoding a pore-forming polypeptide. Neuron 11:433–448.
Lin J, Yan X, Markus A, Redies C, Rolfs A, Luo J. 2010. Expression of seven members of the ADAM family in developing chicken spinal cord. Dev Dyn 239:1246–1254.
Liu BP, Strittmatter SM. 2001. Semaphorin-mediated axonal guidance via Rho-related G proteins. Curr Opin Cell Biol 13:619–626.
Mathey EK, Derfuss T, Storch MK, Williams KR, Hales K, Woolley DR, Al-Hayani A, Davies SN, Rasband MN, Olsson T, Moldenhauer A, Velhin S, Hohlfeld R, Meinl E, Linington C. 2007. Neurofascin as a novel target for autoantibody-mediated axonal injury. J Exp Med 204:2363–2372.
Misgeld T, Kerschensteiner M, Bareyre FM, Burgess RW, Lichtman JW. 2007. Imaging axonal transport of mitochondria in vivo. Nat Methods 4:559–561.
Mitchell KJ, Pinson KI, Kelly OG, Brennan J, Zupicich J, Scherz P, Leighton PA, Goodrich LV, Lu X, Avery BJ, Tate P, Dill K, Pangilinan E, Wakenight P, Tessier-Lavigne M, Skarnes WC. 2001. Functional analysis of secreted and transmembrane proteins critical to mouse development. Nat Genet 28:241–249.
Nave KA, Trapp BD. 2008. Axon-glial signaling and the glial support of axon function. Annu Rev Neurosci 31:535–561.
Norton WT, Poduslo SE. 1973. Myelination in rat brain: Method of myelin isolation. J Neurochem 21:749–757.
Ogawa Y, Rasband MN. 2009. Proteomic analysis of optic nerve lipid rafts reveals new paranodal proteins. J Neurosci Res 87:3502–3510.
Ozkaynak E, Abello G, Jaegle M, van Berge L, Hamer D, Kegel L, Driegen S, Sagane K, Bermingham JR Jr, Meijer D. 2010. Adam22 is a major neuronal receptor for Lgi4-mediated Schwann cell signaling. J Neurosci 30:3857–3864.
Pagliarini DJ, Calvo SE, Chang B, Sheth SA, Vafai SB, Ong SE, Walford GA, Sugiana C, Boneh A, Chen WK, Hill DE, Vidal M, Evans JG, Thorburn DR, Carr SA, Mootha VK. 2008. A mitochondrial protein compendium elucidates complex I disease biology. Cell 134:112–123.
Pedraza L, Fidler L, Staugaitis SM, Colman DR. 1997. The active transport of myelin basic protein into the nucleus suggests a regulatory role in myelination. Neuron 18:579–589.
Pedraza L, Huang JK, Colman DR. 2001. Organizing principles of the axoglial apparatus. Neuron 30:335–344.
Poliak S, Peles E. 2003. The local differentiation of myelinated axons at nodes of Ranvier. Nat Rev Neurosci 4:968–980.
Ricard D, Stankoff B, Bagnard D, Aguera M, Rogemond V, Antoine JC, Spassky N, Zalc B, Lubetzki C, Belin MF, Honnorat J. 2000. Differential expression of collapsin response mediator proteins (CRMP/ULIP) in subsets of oligodendrocytes in the postnatal rodent brain. Mol Cell Neurosci 16:324–337.
Roth AD, Ivanova A, Colman DR. 2006. New observations on the compact myelin proteome. Neuron Glia Biol 2:15–21.
Sagane K, Yamazaki K, Mizui Y, Tanaka I. 1999. Cloning and chromosomal mapping of mouse ADAM11, ADAM22, and ADAM23. Gene 236:79–86.
Salzer JL, Brophy PJ, Peles E. 2008. Molecular domains of myelinated axons in the peripheral nervous system. Glia 56:1532–1540.
Salzer JL, Holmes WP, Colman DR. 1987. The amino acid sequences of the myelin-associated glycoproteins: Homology to the immunoglobulin gene superfamily. J Cell Biol 104:957–965.
Schmidt EF, Strittmatter SM. 2007. The CRMP family of proteins and their role in Sema3A signaling. Adv Exp Med Biol 600:1–11.
Shen S, Sandoval J, Swiss VA, Li J, Dupree J, Franklin RJ, Casaccia-Bonnefil P. 2008. Age-dependent epigenetic control of differentiation inhibitors is critical for remyelination efficiency. Nat Neurosci 11:1024–1034.
Susuki K, Rasband MN. 2008. Molecular mechanisms of node of Ranvier formation. Curr Opin Cell Biol 20:616–623.
Tait S, Gunn-Moore F, Collinson JM, Huang J, Lubetzki C, Pedraza L, Sherman DL, Colman DR, Brophy PJ. 2000. An oligodendrocyte cell adhesion molecule at the site of assembly of the paranodal axo-glial junction. J Cell Biol 150:657–666.
Takamori S, Holt M, Stenius K, Lemke EA, Gronborg M, Riedel D, Urlaub H, Schenck S, Brugger B, Ringler P, Muller SA, Rammner B, Grater F, Hub JS, De Groot BL, Mieskes G, Moriyama Y, Klingauf J, Grubmuller H, Heuser J, Wieland F, Jahn R. 2006. Molecular anatomy of a trafficking organelle. Cell 127:831–846.
Taylor CM, Marta CB, Claycomb RJ, Han DK, Rasband MN, Coetzee T, Pfeiffer SE. 2004. Proteomic mapping provides powerful insights into functional myelin biology. Proc Natl Acad Sci USA 101:4643–4648.
Taylor CM, Pfeiffer SE. 2003. Enhanced resolution of glycosylphosphatidylinositol-anchored and transmembrane proteins from the lipid-rich myelin membrane by two-dimensional gel electrophoresis. Proteomics 3:1303–1312.
Toews JC, Schram V, Weerth SH, Mignery GA, Russell JT. 2007. Signaling proteins in the axoglial apparatus of sciatic nerve nodes of Ranvier. Glia 55:202–213.
Trapp BD, Andrews SB, Wong A, O'Connell M, Griffin JW. 1989. Co-localization of the myelin-associated glycoprotein and the microfilament components, F-actin and spectrin, in Schwann cells of myelinated nerve fibres. J Neurocytol 18:47–60.
Vanrobaeys F, Van Coster R, Dhondt G, Devreese B, Van Beeumen J. 2005. Profiling of myelin proteins by 2D-gel electrophoresis and multidimensional liquid chromatography coupled to MALDI TOF-TOF mass spectrometry. J Proteome Res 4:2283–2293.
Verbisck NV, Costa ET, Costa FF, Cavalher FP, Costa MD, Muras A, Paixao VA, Moura R, Granato MF, Ierardi DF, Machado T, Melo F, Ribeiro KB, Cunha IW, Lima VC, Maciel Mdo S, Carvalho AL, Soares FF, Zanata S, Sogayar MC, Chammas R, Camargo AA. 2009. ADAM23 negatively modulates alpha(v)beta(3) integrin activation during metastasis. Cancer Res 69:5546–5552.
Werner HB, Kuhlmann K, Shen S, Uecker M, Schardt A, Dimova K, Orfaniotou F, Dhaunchak A, Brinkmann BG, Mobius W, Guarente L, Casaccia-Bonnefil P, Jahn O, Nave KA. 2007. Proteolipid protein is required for transport of sirtuin 2 into CNS myelin. J Neurosci 27:7717–7730.
White R, Gonsior C, Kramer-Albers EM, Stohr N, Huttelmaier S, Trotter J. 2008. Activation of oligodendroglial Fyn kinase enhances translation of mRNAs transported in hnRNP A2-dependent RNA granules. J Cell Biol 181:579–586.
Yamaguchi Y, Miyagi Y, Baba H. 2008. Two-dimensional electrophoresis with cationic detergents: A powerful tool for the proteomic analysis of myelin proteins. Part 2: Analytical aspects. J Neurosci Res 86:766–775.